Article:
Zhou, H, Wu, C, Onwudili, JA et al. (3 more authors) (2015) Polycyclic aromatic hydrocarbons (PAH) formation from the pyrolysis of different municipal solid waste fractions. Waste Management, 36. 136 - 146. ISSN 0956-053X

https://doi.org/10.1016/j.wasman.2014.09.014

Polycyclic aromatic hydrocarbons (PAH) formation from the pyrolysis of different municipal solid waste fractions

Hui Zhou[a,b], Chunfei Wu[b,*], Jude A. Onwudili[b], Aihong Meng[a],

Yanguo Zhang[a,*], Paul T. Williams[b,*]

[a] Key Laboratory for Thermal Science and Power Engineering of Ministry of Education, Department of Thermal Engineering, Tsinghua University, Beijing 100084, P.R. China

[b] Energy Research Institute, University of Leeds, Leeds LS2 9JT, UK

ABSTRACT

The formation of 2-4 ring polycyclic aromatic hydrocarbons (PAH) from the pyrolysis of nine different municipal solid waste fractions (xylan, cellulose, lignin, pectin, starch, polyethylene (PE), polystyrene (PS), polyvinyl chloride (PVC), and polyethylene terephthalate (PET)) were investigated in a fixed bed furnace at 800 °C. The mass distribution of pyrolysis was also reported. The results showed that PS generated the most total PAH, followed by PVC, PET, and lignin. More PAH were detected from the pyrolysis of plastics than the pyrolysis of biomass. In the biomass group, lignin generated more PAH than others. Naphthalene was the most abundant PAH, and the amount of 1-methynaphthalene and 2-methynaphthalene was also notable. Phenanthrene and fluorene were the most abundant 3-ring PAH, while benzo[a]anthracene and chrysene were notable in the tar of PS, PVC, and PET. 2-ring PAH dominated all tar samples, and varied from 40 wt.% to 70 wt.%. For PS, PET and lignin, PAH may be generated directly from the aromatic structure of the feedstock.

KEYWORDS: Polycyclic aromatic hydrocarbons (PAH); waste; plastics; biomass; pyrolysis

---

*Corresponding authors. Tel.: +44 1133432504 (P.T. Williams, C. Wu), +86 10 62783373 (Y. Zhang).

E-mail address: p.t.williams@leeds.ac.uk (P.T.Williams), c.wu@leeds.ac.uk (C. Wu), zhangyg@tsinghua.edu.cn (Y. Zhang).

1. Introduction

Large amounts of municipal solid waste (MSW) are generated every year. Properly managed waste treatment is hence an urgent and important task for the sustainable development of cities (Cheng and Hu, 2010; Rada, 2014). Waste to energy (WTE) through incineration is an established technology; however, pyrolysis and gasification are advanced thermal treatment technologies receiving increasing attention for the treatment of MSW (Cheng et al., 2007; Zhou et al., 2014a; Arena et al., 2012; Ionescu et al., 2013). The products of pyrolysis and gasification (oil, char and syngas) allow for a broad range of applications e.g. electricity and heat production from combustion of syngas gas; chemicals and transportation fuels extracted from liquid pyrolysis oils (Liu and Liu, 2005; Hanaoka et al., 2005). In the process of pyrolysis and gasification, thermal-decomposition of the raw materials (pyrolysis) is considered to be a fundamental process (Zhou et al., 2013). Therefore, fundamentally understanding the MSW pyrolysis process is an important topic for the thermal conversion of MSW.

One of the challenges for the development of thermal processing of MSW is the production of pollutants such as polycyclic aromatic hydrocarbons (PAH) (Rochman et al., 2013; Hajizadeh et al., 2011). There is some concern over the emissions of PAH in the environment (Sun et al., 1998), since they are associated with human teratogenesis, cancer or mutations, with a bioaccumulative effect (Samanta et al., 2002; Moeckel et al., 2014; Ionescu et al., 2012). In addition, one of the main formation pathways for polychlorinated dibenzo-p-dioxins and dibenzofurans (PCDD/Fs) is from organic precursors in the fly ash, and PAH in fly ash is most likely involved in PCDD/Fs formation as an intermediate reactant (Iino et al., 1999; Fullana et al., 2005; Chin et al., 2012). Further, fine particulates with a diameter equal to or below 2.5 μm

generated from the thermal conversion of MSW can be passed more deeply into the lungs (Miller et al., 1979; Ragazzi et al., 2013; Buonanno et al., 2011) and fine particulates are also suggested to be associated with PAH (Richter et al., 2000). Therefore, understanding the emissions of PAH is an important research topic.

Although hundreds of PAH exist in the environment, only 16 PAH, i.e. naphthalene, acenaphthylene, acenaphthene, fluorene, phenanthrene, anthracene, fluoranthene, pyrene, benzo[a]anthracene, chrysene, benzo[b]fluoranthene, benzo[k]fluoranthene, benzo[a]pyrene, dibenzo[a,h]anthracene, benzo[g,h,i]perylene, and indeno[1,2,3-cd]pyrene, have been selected by the US Environmental Protection Agency (US EPA) as priority pollutants, which are monitored routinely for regulatory purposes (OFR, 2000).

There have been investigations of tar production, including PAH, from pyrolysis of biomass or MSW (Wu et al., 2013; Onwudili et al., 2009; Li et al., 2013; Marsh et al., 2004; McGrath et al., 2003). For example, we have previously studied the pyrolysis of xylan, cellulose and lignin in a two-stage reactor system with or without the presence of nickel-based catalysts. Naphthalene was identified in all samples, and the highest concentration of naphthalene was obtained for the pyrolysis of lignin without a catalyst. Various kinds of PAH were found only in the tar from the pyrolysis of lignin (Wu et al., 2013). The pyrolysis of low-density polyethylene (LDPE) was investigated in a closed batch autoclave reactor under an inert nitrogen atmosphere. Compositional analysis of the oil products showed that for the pyrolysis of LDPE, aliphatic hydrocarbons were the major components, but the proportion of aromatic compounds including naphthalene increased with the increase of reaction temperature and residence times (Onwudili et al., 2009). The results of Li et al. (2013) show that the pyrolysis of cellulose generated more naphthalene (3.87%) than the pyrolysis of LDPE (0.79%) in the presence of ZSM-5 catalyst

using a Py-GC/MS reaction system at 650°C. McGrath et al. (2003) investigated the formation of PAH from the pyrolysis of cellulose over the temperature range of 300-650°C. Detectable amounts of 2-4 ring PAH were observed at and above 400°C. The pathway to PAH formation in the 300-650°C temperature range was believed to proceed via the carbonization process where the solid residue underwent a chemical transformation and rearrangement to give a more condensed polycyclic aromatic structure. However, it appears that most of the work reported in the literature has focused on only a small number of components (Wu et al., 2013; Onwudili et al., 2009; Li et al., 2013; Marsh et al., 2004; McGrath et al., 2003). There are few reports investigating the release of PAH from a large range of MSW fractions.

MSW is a very complicated material including plastics and lignocellulosic biomass etc. (Zhou et al., 2014b; Burnley, 2007). Therefore, model pure compounds representing MSW, such as cellulose, lignin, PE, and PVC, have been researched to understanding the mechanism of pyrolysis (Luo et al., 2010; Yang et al., 2007). However, it is difficult to compare the influence of MSW raw materials on the release of PAH from a review of the literature due to the range of different raw materials investigated, different reactor types and reaction conditions. Therefore, using representative MSW fractions investigating a large range of PAH in the same reactor and identical reaction conditions, will give information about PAH formation during the thermal conversion of MSW.

In this paper, nine MSW fractions including hemi-cellulose, cellulose, lignin, pectin, starch, polyethylene (PE), polystyrene (PS), polyvinyl chloride (PVC), and polyethylene terephthalate (PET) were investigated. The formation of PAH from the pyrolysis of the chosen fractions is presented and discussed together with the production of gas and solid reside products.

2. Materials and methods

2.1. Materials

Xylan (commonly representative of hemi-cellulose, from beech wood), starch (from rice), lignin (alkaline), and PVC were obtained from Sigma-Aldrich. Cellulose (microcrystalline) was provided from Research Chemicals Ltd. PE and PS were purchased from Goodfellow Cambridge Ltd., while pectin (citrus) and PET were provided from Alfa Aesar and Shanghai Yangli Mechanical and Electrical Technology Co., Ltd., respectively. All the samples were in granular form of particle size less than 150 μm. Results of the proximate and ultimate analysis of the samples are shown in Table 1.

The nine samples were divided into 2 groups, xylan, cellulose, lignin, pectin, and starch which can be regarded as a biomass sample group, and PE, PS, PVC, and PET can be regarded as a plastic sample group. In the biomass group, lignin (Table 1) showed the highest fixed carbon content (32.60 wt.%) and elemental carbon content (61.33 wt.%), and the lowest volatile content (60.37 wt.%) and oxygen content (31.71 wt.%). A significant amount of sulphur (0.69 wt.%) was also found in the lignin sample. In addition, cellulose showed the highest volatile content (93.37 wt.%), the lowest ash content (0.07 wt.%) and fixed carbon content (1.89 wt.%). Xylan had a notable amount of nitrogen (2.70 wt.%). The high volatile content of cellulose and high sulphur content of lignin have been reported by other researchers (Couhert et al., 2009; Yoon et al., 2012). For the plastic group, the volatiles content were all very high; PVC and PET have a certain amount of fixed carbon. PE has the highest hydrogen content (11.20 wt.%), and PS has the highest nitrogen content (5.73 wt.%). The chlorine content of PVC is as high as 56.35 wt.%, while the oxygen content of PET is 32.64 wt.%.

2.2. Pyrolysis process

Pyrolysis of the samples was carried out using a fixed-bed reactor system (Fig. 1). The system was composed of a pyrolysis reactor, tar collection system and gas collection stages. During the experiment, N_2 (100 ml min^{-1}) was used as carrier gas, and the residence time of volatiles was approximately 2.6 s. During the experiment, the reactor was initially heated to the set point (800 °C). Once the temperature had stabilized, the sample (1 g) was inserted into the hot zone of the reactor and rapidly pyrolysed. The average heating rate was approximately 350 °C min^{-1}, which was a rough evaluation of how fast the sample was heated. The reactor was kept at the reaction temperature for a further 30 min. The products from the pyrolysis were cooled using air and dry ice cooled condensers, thereby collecting the condensed tar. The non-condensed gases were collected using a Tedlar™ gas bag, and further analysed off-line using packed column gas chromatography (GC). An additional 20 min was allowed to collect the non-condensed gases to ensure complete collection of gas products. For the pyrolysis of PVC, the generated HCl was absorbed by an additional scrubber/condenser system placed between the existing condensers and the gas sample bag. The additional system consisted of a water bubbler/scrubber to absorb the HCl followed by a dry ice condenser. All experiments were repeated to ensure the reliability of the results.

2.3. Products analysis and characterization

Non-condensed gases collected in the Tedlar™ gas sample bag were analysed off-line by packed column gas chromatography. H_2, CO and N_2 were analysed with a Varian 3380 GC on a 60–80 mesh molecular sieve column with argon carrier gas, whilst CO_2 was analysed by another Varian 3380 GC on a Hysep 80–100 mesh column with argon carrier gas. C_1-C_4 hydrocarbons were analysed using a third Varian 3380 gas chromatograph with a flame ionisation detector, with an 80–100 mesh Hysep column and nitrogen carrier gas. From the known volume of N_2 calculated from the flow rate and collection time, the volume and mass of other gases can be calculated.

After every experiment, the condenser and the tar connecting sections were weighed to obtain the mass of tar (weight difference of the condensation system). The collected tar samples were recovered from the condensers by the use of different solvents to enable an initial separation of aliphatic and aromatic compounds. The tar products from the condensers were washed by firstly hexane, which removes all the aliphatic compounds and a part of the aromatic fraction of the tar. Secondly, the condensers were washed using ethyl acetate to collect the residual aromatic compounds. The water content in the liquid mixture was eliminated by filtering through a column of anhydrous sodium sulphate. The aliphatic and aromatic compounds in the hexane were separate by a packed column containing a mixture of silica and alumina sorbent, designed to fractionate aliphatic and aromatic compounds. The hexane solution went through the column first, followed by ethyl acetate. The column was obtained from Biotage Ltd, UK and had been designed to fractionate aliphatic and aromatic compounds from petroleum hydrocarbons, the column. was designed for 50 ml oil, and the diameter was approximate 2 cm.

Finally, the aromatic oil fractions (from both hexane and ethyl acetate), which contained PAH, were analysed using a Varian CP-3800 gas chromatograph coupled with a Varian Saturn

2200 mass spectrometer (GC/MS) fitted with a 30m × 0.25μm DB-5 equivalent column. 2 μl of the extracted tar sample was injected into the GC injector port at a temperature of 290 °C; the oven programme temperature was at 50 °C for 6 min, then ramped to 210 °C at 5 °C min^{-1}, held for 1 min and ramped at 8°C min^{-1} to 300 °C (total analysis time of 61 min). The transfer line was at 280 °C, manifold at 120 °C and the ion trap temperature was held at 220 °C. The ion trap was initially switched off for 7 min to allow the elution of the solvent prior to data acquisition to safeguard the life of the trap. The PAH compounds present in the tars were quantified by internal standard method with 2-hydoxyacetophenone as internal standard (IS). The GC/MS was calibrated by standard PAH supplied by Sigma-Aldrich Ltd., thus PAH could be quantitatively determined. The analysis reported 10 of the 2-4-ring PAH from US EPA priority list and also 2 naphthalene derivatives (1-methylnaphthalene and 2-methylnaphthalene). The GC peaks of benzo[a]anthracene and chrysene could not be separated clearly by the GC system used; therefore the concentration of these two compounds was reported together.

3. Results

3.1. Mass balance

The mass balance for the pyrolysis of the different MSW samples is shown in Table 2. The mass balance was calculated as the mass of outputs (tar, gas and residue) divided by the mass of inputs (sample). Gas yield was obtained by the mass of non-condensed gases (calculated from the GC analysis) divided by the sample (1 g). The residue fraction was calculated by the

mass of residue after pyrolysis in the reactor divided by the sample mass. Tar yield was calculated as the mass of the collected tar from the condensers divided by the sample mass.

As shown in Table 2, for the biomass type samples, cellulose and starch produced the highest gas yield (62.2 wt.%), and lignin produced the lowest gas yield (30.4 wt.%). Xylan produced the highest tar yield (37.6 wt.%), and lignin produced the lowest tar yield (25.8 wt.%). In addition, lignin produced the highest residue (33.3 wt.%), which was consistent with the fixed carbon and ash content of the sample, as shown in Table 1. The high content of volatiles from the decomposition of cellulose and the lowest volatiles content from the decomposition of lignin have also been reported by others using thermogravimetric analysis (TGA) (Zhou et al., 2013; Yang et al., 2007). It could be noticed that cellulose and starch had similar mass distribution, which might be due to their similar compositions based on the monomer of glucose (Dumitriu, 2004; Shafizadeh et al., 1973).

For the plastic samples, PE, PVC and PET produced the highest gas yield, and PS produced the lowest gas yield (5.7 wt.%). Consequently, PS produced the highest tar yield (84.3 wt.%). The high tar yield from the pyrolysis of PS was also reported by Scott et al. (1990). The pyrolysis of PVC generated 38.5 wt.% HCl, which is also included in the gas yield in Table 2. The HCl content was lower than the chlorine content (56.35 wt.%) of PVC in Table 1, indicating that chlorine participated in the formation of compounds of tar or solid. The chlorine in tar in the form of various chlorobenzenes was detected by Iida et al. (1974) at 700 °C using a pyrolysis gas chromatograph.

3.2. PAH analysis

3.2.1. Discussion of PAH in terms of biomass and plastic components

PAH present in the tar derived from the pyrolysis process were analysed quantitatively by GC/MS. The PAH generation from pyrolysis of different samples are shown in Fig. 2. It can be seen that, plastics, especially PS and PVC, generated a large amount of PAH. PS generated the most naphthalene (12460 µg/g sample), fluorene (2540 µg/g sample), phenanthrene (6001µg/g sample), anthracene (1275 µg/g sample), fluoranthene (380 µg/g sample), and pyrene (354 µg/g sample), while PVC generated the most 1-methynaphthalene (922 µg/g sample), 2-methynaphthalene (1059 µg/g sample), acenaphthylene (377 µg/g sample), acenaphthene (50 µg/g sample), and benzo[a]anthracene plus chrysene (1490 µg/g sample).

The tar resulting from PE pyrolysis showed the presence of naphthalene, methylnaphthalene, acenaphthylene, acenaphthene, fluorene, and phenanthrene; these PAH have also been confirmed in the tar sample collected from pyrolysis of PE at 700 °C in a fluidized bed reactor (Williams and Williams, 1999).

In the biomass group of model compounds, lignin generated a certain amount of several PAH except anthracene. Another important biomass component, cellulose produced only a small amount of naphthalene, 1-methynaphthalene, 2-methynaphthalene, acenaphthylene, fluorene, phenanthrene, and anthracene, which has also been reported by Stefanidis et al. (2014). The pyrolysis of pectin produced naphthalene, 1-methynaphthalene, 2-methynaphthalene, acenaphthylene, fluorene, phenanthrene, pyrene, and benzo[a]anthracene plus chrysene. Comparing the pyrolysis of pectin at 600-800 °C reported by McGrath et al. (2001), the PAH produced in this work showed more naphthalene, acenaphthylene, fluorene, phenanthrene, and pyrene, while anthracene and fluoranthene were not detected. The pyrolysis of xylan generated

naphthalene, 1-methynaphthalene, 2-methynaphthalene, acenaphthylene, acenaphthene, fluorene, and phenanthrene, while anthracene, fluoranthene, pyrene, and benzo[a]anthracene were not detected. However, Yu et al. (2014) reported the presence of anthracene, fluoranthene, pyrene, and benzo[a]anthracene from the pyrolysis of xylan with an excess air ratio 0.2 in a entrained-flow gasification reactor.

Fig. 2 (l) shows the total 2-4 ring PAH found in the tars from pyrolysis of the model MSW compounds. PS generated the most total PAH, followed by PVC, PET, lignin, and PE. Generally, plastics release more PAH during the pyrolysis process than biomass.

3.2.2. Discussion of PAH in terms of number of rings

Naphthalene, which is the simplest PAH, was also the most abundant PAH in the tar. The high naphthalene content of PVC pyrolysis was also reported by other researchers (Iida et al, 1974). Two methyl derivatives of naphthalene (Fig.2 (b) and (c)) were also presented in the tar at considerable concentrations, and the amount present was quite similar. Phenanthrene and fluorene were the most abundant 3-ring PAH in pyrolysis tar, while the amount of acenaphthene was small, and anthracene was only found in the tar of PS and PVC. Two 4-ring PAH, benzo[a]anthracene and chrysene, are notably present in the tar of PS, PVC, and PET.

The percentage of 2-ring, 3-ring, and 4-ring PAH for every sample was calculated as the total mass of 2-ring, 3-ring, and 4-ring PAH divided by the total mass of 2-4 ring PAH, and the results are shown in Fig. 3. 2-ring PAH were dominant for all samples. Especially for PE, the percentage of 2-ring PAH was about 90 wt.%. For other samples, the percentage of 2-ring PAH varied from 40 wt.% to 70 wt.%. It was difficult to detect 4-ring PAH in the tar derived from

pyrolysis of xylan, cellulose, and PE, while the percentage of 4-ring PAH was between 5 wt.% and 25 wt.% for other samples.

4. Discussion of PAH formation

4.1. Mechanism of components degradation to PAH precursors

The formation of PAH has various routes. Among several reported mechanisms, hydrogen abstraction acetylene addition (HACA) is widely accepted (Shukla and Koshi, 2012). As shown in (R1), naphthalene can be generated from benzene via phenylacetylene, which is abundant in the tar sampled produced in this work.

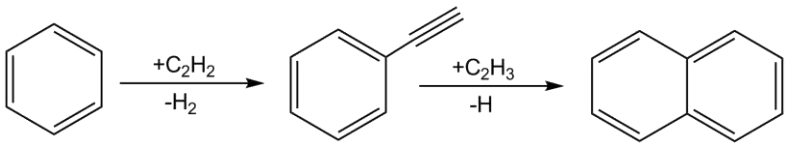

(R1)

Therefore, single-ring compounds (such as benzene and styrene) can be regarded as PAH precursors. For those samples that have aromatic rings, such as PS, PET and lignin, PAH may be generated from the aromatic structure via the HACA mechanism (Mastral and Callén, 2000; Shukla and Koshi, 2012). Among these three samples, the aromatic ring mass percentage of PS is the largest, and that might be responsible for the production of the highest concentration of PAH from the PS pyrolysis (Fig. 2). In addition, styrene is identified as a major product in the tar of PS pyrolysis. The thermal degradation mechanism for PS has been shown to begin with chain scission, followed by additional scission steps (Wang et al., 2003). As reported by Shukla and Koshi (2012), the conversion of styrene into phenylacetylene by hydrogen elimination is highly probable. And further addition of C_2H_3 to phenylacetylene at the ortho position resulting in

naphthalene is also possible, as shown in (R2). That might be responsible for the highest production of the most PAH from the PS pyrolysis.

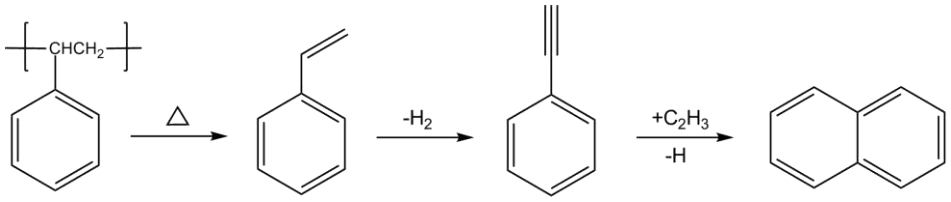

(R2)

Monomers (such as guaiacols and syringols with alkyls) were generated initially from the lignin pyrolysis. Then through the process of dehydroxylation and demethoxylation, derivatives of benzenes were formed, and the process of demethylation occurred simultaneously. Asmadi et al. (2011a, 2011b) reported that the thermal decomposition of lignin begins by cleavage of the weak α-ether and β-ether bonds of the lignin structure, which releases guaiacyl- and syringyl-type aromatics. These aromatics further react to produce catechols and pyrogallols, which can be decomposed to form PAH. The process of lignin decomposition is shown in Fig. 4, where coniferyl alcohol monomer is taken as an example.

PAH of the pyrolysis of PE are formed through secondary reactions via Diels-Alder type reactions involving alkenes and di-alkenes to form benzenes (Cypres, 1987; Williams and Williams, 1999; Depeyre et al., 1985; Fairburn et al., 1990). It should be noted that formation of styrene and phenylacetylene from aliphatic species by reactions R3 and R4 cannot be neglected (Shulka and Koshi, 2012).

$C_4H_5 + C_4H_4 \rightarrow C_8H_8 + H$ (R3)

$C_4H_5 + C_4H_2 \rightarrow C_8H_6 + H$ (R4)

As shown in Fig. 2, the pyrolysis of PVC formed much more PAH than the pyrolysis of PE. Aliphatic hydrocarbons could be hardly detected in the tar produced from PVC pyrolysis, and the yield of alkenes in the gas product was also very low. It is suggested that aromatic rings

may be formed directly from the chain scission process after the dehydrochlorination process of PVC molecules, bypassing the process of the Diels-Alder reaction. As reported by Gui et al. (2013), the content of 2-ring group aromatics increased from 7.02 to 31.75% with increasing peak temperature from 500 to 800 °C during PVC pyrolysis; at a longer holding time of 300 s, an increase of 2 rings group aromatics from 7.02 to 50.33% was also observed in tar derived from pyrolysis of PVC at 500 °C. It seems that 3-4 rings compounds were formed in the early stage and then 2-ring compounds were released in the later stage of PVC pyrolysis. Therefore, a new four-stage mechanism was proposed, including (1) dechlorination accompanied with inner cyclization, (2) aromatic chain scission, (3) release of quasi-3 rings or 3 rings group, and (4) release of 2 rings group, of the PVC tar formation, as shown in Fig. 5 (Jordan et al., 2001). In the PVC pyrolysis experiment, large amounts of soot were generated, which verified this mechanism.

It has been reported that the formation of PAH from biomass pyrolysis at high temperature and long residence times was attributed to two mechanisms: Diels-Alder type reactions, and the deoxygenation of oxygenated aromatic compounds (Williams and Horne, 1995). However, low concentrations of alkenes and di-alkenes were detected in the gas and tar products from pyrolysis. It was unlikely that Diels-Alder type reactions would take place during the pyrolysis of biomass samples. The formation of PAH from pyrolysis of xylan, cellulose, starch, and pectin may follow the same route with benzenes and cyclopentadiene (CPD) as intermediates (Stefanidis et al., 2014). Benzenes with different alkyl substitutions are clearly detected in the tar of these samples.

4.2. Mechanism of PAH growth

Heavier molecular weight PAH may form from lighter molecular weight PAH and single-ring compounds. The preferred production of large PAH, either benzenoid-PAH (Bz-PAH) or cyclopentaring-fused PAH (CP-PAH), depends on growth pathways from naphthalene. Naphthalene was the most abundant PAH in the tar, as shown in Fig. 2.

Acenaphthylene is expected to be formed from the addition of acetylene to naphthalene, which is supported by the observation of ethenylnaphthalene (Kim et al., 2010). For all samples, the yield of acenaphthylene was higher than that of acenaphthene, which was consistent with the results of ethylene pyrolysis (Shulka and Koshi, 2012). It is likely that acenaphthene is formed from acenaphthylene, as shown in Fig. 6. It was reported that further growth of large PAH via HACA from acenaphthylene was possible (Shulka and Koshi, 2012). Wang and Violi (2006) reported that the 1,2 double bond in acenaphthylene is much more reactive than the 3,4 and 4,5 aromatic bonds, based on which it is easy to explain the formation of fluoranthene, as shown in Fig. 6.

The formation of a new six-member ring via this mechanism can account for ~25% of the total product yield, whereas the remaining ~75% of the products are CP-PAH molecules formed via a five-member ring closure involving the same ethynyl and ethenyl groups (Kislov et al., 2013). Richter and Howard (2000) and Marsh and Wornat (2000) also reported that it is unlikely to produce phenanthrene from naphthalene via HACA.

However, as shown in Fig. 2 (g) and (h), the amounts of phenanthrene and anthracene are considerable. There might be another way to generate Bz-PAH. As reported by Lu and Mulholland, Bz-PAH can be generated from the interaction of naphthalene/CPD (cyclocpentadiene) or CPD/indene, as shown in and Fig. 7 and 8, respectively. Due to the low

boiling point, CPD cannot be detected in the tar, while large amounts of indene are detected in the pyrolysis tar of all the samples except PE.

In the tar produced from pyrolysis of different samples, the amount of phenanthrene was much higher than that of anthracene, which is consistent with the research of others, where the yield of phenanthrene exhibits an order of magnitude higher concentration than anthracene (Kislov et al., 2013). As shown in Fig. 7, CPD can substitute at the α or β position of naphthalene. The selectivity for α over β substitution can be rationalized in terms of the resonance structures of the intermediate: for α substitution intermediate, seven resonance structures can be drawn, of which four preserve an aromatic ring. For β substitution, the intermediate has only six resonance structures, and only two of these are aromatic. α substitution may generate phenanthrene, β substitution may generate anthracene, as shown in Fig. 7. Therefore, phenanthrene formation is preferred to anthracene in the tar, as shown in Fig. 2 (g) and (h).

The PAH distribution pattern are similar for all the samples other than PE, as shown in Fig. 3. PE generates large amounts of naphthalene and some acenaphthylene and acenaphthene, while the yields of phenanthrene and anthracene are very low, indicating that HACA process happens, but the reaction routes shown in Fig. 7 and 8 might not occur. Indene could not be detected in the tar of PE pyrolysis, which supports the above hypothesis.

For the pyrolysis of all the samples, the amounts of 1-methylnaphthalene and 2-methylnaphthalene were lower than that of naphthalene. Shukla and Koshi (2012) reported that the observation of low concentrations of large PAH with aliphatic chains might be because of their faster consumption to form thermally more stable products or soot. Chung and Violi (2011) have also reported that aromatics with attached aliphatic chains show considerably faster

nucleation rates than the corresponding polycyclic aromatic hydrocarbons of similar mass without any chain.

5. Conclusions

Hemi-cellulose, cellulose, lignin, pectin, starch, PE, PS, PVC, and PET, as representative of MSW, were pyrolysed in a fixed bed reactor at 800 °C and the production of PAH in the product tar was investigated. It was found that of the biomass fractions, cellulose and starch produced the highest gas yield, while xylan produced the highest tar yield. The plastics PE, PVC and PET produced the highest gas yield, while PS produced the highest tar yield.

The highest generation of PAH was found from the pyrolysis of PS and PVC. Naphthalene (2-ring) was the most abundant PAH and phenanthrene and fluorene were the most abundant 3-ring PAH, while the 4-ring benzo[a]anthracene and chrysene were found in significant concentrations in the tar of PS, PVC, and PET.

The data suggest that PAH may be generated directly from the aromatic structure for PS, PET and lignin. PAH generated from PE may be via Diels-Alder type reactions, while it seems that aromatic rings may be formed directly from chain scission process after dehydrochlorination process of PVC molecules. For the biomass type model compounds (xylan, cellulose, starch, and pectin), PAH formation may follow the same route with benzenes and cyclopentadiene (CDP) as intermediates. PAH may grow via HACA mechanisms, or from the interaction of naphthalene/CPD or CDP/indene.

Acknowledgments

The financial support from National Basic Research Program of China (973 Program, No. 2011CB201502) is gratefully acknowledged.

References

Arena, U., 2012. Process and technological aspects of municipal solid waste gasification. A review. Waste Manage. 32, 625-639.

Asmadi, M., Kawamoto, H., Saka, S., 2011a. Thermal reactions of guaiacol and syringol as lignin model aromatic nuclei. J. Anal. Appl. Pyrol. 92, 88-98.

Asmadi, M., Kawamoto, H., Saka, S., 2011b. Thermal reactivities of catechols/pyrogallols and cresols/xylenols as lignin pyrolysis intermediates. J. Anal. Appl. Pyrol. 92, 76-87.

Buonanno, G., Stabile, L., Avino, P., Belluso, E., 2011. Chemical, dimensional and morphological ultrafine particle characterization from a waste-to-energy plant, Waste Manage., 31(11), 2253-2262.

Burnley, S.J., 2007. A review of municipal solid waste composition in the United Kingdom. Waste Manage. 27, 1274-1285.

Cheng, H.F., Zhang, Y.G., Meng, A.H., Li, Q.H., 2007. Municipal solid waste fueled power generation in china: a case study of waste-to-energy in changchun city. Environ. Sci. Technol. 41, 7509-7515.

Cheng, H.F., Hu, Y.N., 2010. Municipal solid waste (MSW) as a renewable source of energy: Current and future practices in China. Bioresource Technol. 101, 3816-3824.

Chin, Y., Lin, C., Guo-Ping, C., Yu-Min, W., 2012. PCDD/F Formation Catalyzed by the Metal Chlorides and Chlorinated Aromatic Compounds in Fly Ash. Aerosol Air Qual. Res. 12, 228-236.

Chung, S., Violi, A., 2011. Peri-condensed aromatics with aliphatic chains as key intermediates for the nucleation of aromatic hydrocarbons. P. Combust. Inst. 33, 693-700.

Couhert, C., Commandre, J.M., Salvador, S., 2009. Is it possible to predict gas yields of any biomass after rapid pyrolysis at high temperature from its composition in cellulose, hemicellulose and lignin? Fuel 88, 408-417.

Cypres, R., 1987. Aromatic hydrocarbons formation during coal pyrolysis. Fuel Process. Technol. 15, 1-15.

Depeyre, D., Flicoteaux, C., Chardaire, C., 1985. Pure n-hexadecane thermal steam cracking. Ind. Eng. Chem. Process Des. Dev. 24, 1251-1258.

Dumitriu, S., 2004. Polysaccharides: Structural Diversity and Functional Versatility, 2nd. CRC Press, Boca Raton, Florida.

Fairburn, J.A., Behie, L.A., Svrcek, W.Y., 1990. Ultrapyrolysis of n-hexadecane in a novel micro-reactor. Fuel 69, 1537-1545.

Fullana, A., Sidhu, S.S., 2005. Fate of PAH in the post-combustion zone: Partial oxidation of PAH to dibenzofuran over CuO. J. Anal. Appl. Pyrol. 74, 479-485.

Gui, B., Qiao, Y., Wan, D., Liu, S., Han, Z., Yao, H., Xu, M., 2013. Nascent tar formation during polyvinylchloride (PVC) pyrolysis. P. Combust. Inst. 34, 2321-2329.

Hajizadeh, Y., Onwudili, J.A., Williams, P.T., 2011. PCDD/F formation from oxy-PAH precursors in waste incinerator flyash. Chemosphere 85, 1672-1681.

Hanaoka, T., Inoue, S., Uno, S., Ogi, T., Minowa, T., 2005. Effect of woody biomass components on air-steam gasification. Biomass Bioenerg. 28, 69-76.

Iida, T., Nakanishi, M., Got O, K., 1974. Investigations on poly (vinyl chloride). I. Evolution of aromatics on pyrolysis of poly (vinyl chloride) and its mechanism. J. Polym. Sci. Pol. Chem. 12, 737-749.

Iino, F., Imagawa, T., Takeuchi, M., Sadakata, M., 1999. De novo synthesis mechanism of

polychlorinated dibenzofurans from polycyclic aromatic hydrocarbons and the characteristic isomers of polychlorinated naphthalenes. Environ. Sci. Technol. 33, 1038-1043.

Ionescu, G., Zardi, D., Tirler, W., Rada, E.C., Ragazzi, M., 2012. A critical analysis of emissions and atmospheric dispersion of pollutants from plants for the treatment of residual municipal solid waste. UPB Sci. Bull., Serie. D 74, 227-240.

Ionescu, G., Rada, E.C., Ragazzi, M., Mărculescu, C., Badea, A., Apostol, T., 2013. Integrated municipal solid waste scenario model using advanced pretreatment and waste to energy processes. Energ. Convers. Manage. 76, 1083-1092.

Jordan, K.J., Suib, S.L., Koberstein, J.T., 2001. Determination of the Degradation Mechanism from the Kinetic Parameters of Dehydrochlorinated Poly(vinyl chloride) Decomposition. J. Phys. Chem. B 105, 3174-3181.

Kim, D.H., Mulholland, J.A., Wang, D., Violi, A., 2010. Pyrolytic Hydrocarbon Growth from Cyclopentadiene. J. Phys. Chem. A 114, 12411-12416.

Kislov, V.V., Sadovnikov, A.I., Mebel, A.M., 2013. Formation Mechanism of Polycyclic Aromatic Hydrocarbons beyond the Second Aromatic Ring. J. Phys. Chem. A 117, 4794-4816.

Li, X., Zhang, H., Li, J., Su, L., Zuo, J., Komarneni, S., Wang, Y., 2013. Improving the aromatic production in catalytic fast pyrolysis of cellulose by co-feeding low-density polyethylene. Appl. Catal. A-Gen. 455, 114-121.

Liu, Y.S., Liu, Y.S., 2005. Novel incineration technology integrated with drying, pyrolysis, gasification, and combustion of MSW and ashes vitrification. Environ. Sci. Technol. 39, 3855-3863.

Luo, S.Y., Xiao, B., Hu, Z.Q., Liu, S.M., 2010. Effect of particle size on pyrolysis of single-component municipal solid waste in fixed bed reactor. Int. J. Hydrogen Energ. 35, 93-97..

Marsh, N.D., Wornat, M.J., 2000. Formation pathways of ethynyl-substituted and cyclopenta-fused polycyclic aromatic hydrocarbons. P. Combust. Inst. 28, 2585-2592.

Marsh, N.D., Ledesma, E.B., Sandrowitz, A.K., Wornat, M.J., 2004. Yields of Polycyclic Aromatic Hydrocarbons from the Pyrolysis of Catechol [ortho-Dihydroxybenzene]: Temperature and Residence Time Effects. Energ. Fuel. 18, 209-217.

Mastral, A.M., Callén, M.S., 2000. A Review on Polycyclic Aromatic Hydrocarbon (PAH) Emissions from Energy Generation. Environ. Sci. Technol. 34, 3051-3057.

Mcgrath, T., Sharma, R., Hajaligol, M., 2001. An experimental investigation into the formation of polycyclic-aromatic hydrocarbons (PAH) from pyrolysis of biomass materials. Fuel 80, 1787-1797.

Mcgrath, T.E., Chan, W.G., Hajaligol, M.R., 2003. Low temperature mechanism for the formation of polycyclic aromatic hydrocarbons from the pyrolysis of cellulose. J. Anal. Appl. Pyrol. 66, 51-70.

Miller, F.J., Gardner, D.E., Graham, J.A., Lee, R.E., Wilson, W.E., Bachmann, J.D., 1979. Size Considerations for Establishing a Standard for Inhalable Particles. J. Air Pollut. Control 29, 610-615.

Moeckel, C., Monteith, D.T., Llewellyn, N.R., Henrys, P.A., Pereira, M.G., 2014. Relationship between the Concentrations of Dissolved Organic Matter and Polycyclic Aromatic Hydrocarbons in a Typical U.K. Upland Stream. Environ. Sci. Technol. 48, 130-138.

Office of the Federal Register (OFR), 2000. Code of Federal Regulations, U.S. Government Printing Office, Washington.

Onwudili, J.A., Insura, N., Williams, P.T., 2009. Composition of products from the pyrolysis of polyethylene and polystyrene in a closed batch reactor: Effects of temperature and residence time. J. Anal. Appl. Pyrol. 86, 293-303.

Rada, E.C., 2014. Energy from municipal solid waste. WIT T. Ecol. Environ. 190, 945-957.

Ragazzi, M., Tirler, W., Angelucci, G., Zardi, D., Rada, E.C., 2013. Management of atmospheric pollutants from waste incineration processes: The case of Bozen, Waste Manage. Res. 31(3), 235-240.

Richter, H., Howard, J., 2000. Formation of polycyclic aromatic hydrocarbons and their growth to soot—a review of chemical reaction pathways. Prog. Energ. Combust. 26, 565-608.

Rochman, C.M., Manzano, C., Hentschel, B.T., Simonich, S.L.M., Hoh, E., 2013. Polystyrene Plastic: A Source and Sink for Polycyclic Aromatic Hydrocarbons in the Marine Environment. Environ. Sci. Technol. 47, 13976-13984.

Samanta, S.K., Singh, O.V., Jain, R.K., 2002. Polycyclic aromatic hydrocarbons: environmental pollution and bioremediation. Trends Biotechnol. 20, 243-248.

Scott, D.S., Czernik, S.R., Piskorz, J., Radlein, D.S.A.G., 1990. Fast pyrolysis of plastic wastes. Energ. Fuel. 4, 407-411.

Shafizadeh, F., Fu, Y.L., 1973. Pyrolysis of cellulose. Carbohyd. Res. 29, 113-122.

Shukla, B., Koshi, M., 2012. A novel route for PAH growth in HACA based mechanisms. Combust. Flame 159, 3589-3596.

Stefanidis, S.D., Kalogiannis, K.G., Iliopoulou, E.F., Michailof, C.M., Pilavachi, P.A., Lappas, A.A., 2014. A study of lignocellulosic biomass pyrolysis via the pyrolysis of cellulose, hemicellulose and lignin. J. Anal. Appl. Pyrol. 105, 143-150.

Sun, F., Littlejohn, D., David Gibson, M., 1998. Ultrasonication extraction and solid phase

extraction clean-up for determination of US EPA 16 priority pollutant polycyclic aromatic hydrocarbons in soils by reversed-phase liquid chromatography with ultraviolet absorption detection. Anal. Chim. Acta 364, 1-11.

Wang, Z., Wang, J., Richter, H., Howard, J.B., Carlson, J., Levendis, Y.A., 2003. Comparative Study on Polycyclic Aromatic Hydrocarbons, Light Hydrocarbons, Carbon Monoxide, and Particulate Emissions from the Combustion of Polyethylene, Polystyrene, and Poly(vinyl chloride). Energ. Fuel. 17, 999-1013.

Wang, D., Violi, A., 2006. Radical−Molecule Reactions for Aromatic Growth: A Case Study for Cyclopentadienyl and Acenaphthylene. J. Org. Chem. 71, 8365-8371.

Williams, P., Horne, P.A., 1995. Analysis of aromatic hydrocarbons in pyrolytic oil derived from biomass. J. Anal. Appl. Pyrol. 31, 15-37.

Williams, P.T., Williams, E.A., 1999. Fluidised bed pyrolysis of low density polyethylene to produce petrochemical feedstock. J. Anal. Appl. Pyrol. 51, 107-126.

Wu, C.F., Wang, Z.C., Huang, J., Williams, P.T., 2013. Pyrolysis/gasification of cellulose, hemicellulose and lignin for hydrogen production in the presence of various nickel-based catalysts. Fuel 106, 697-706.

Yang, H., Yan, R., Chen, H., Lee, D.H., Zheng, C., 2007. Characteristics of hemicellulose, cellulose and lignin pyrolysis. Fuel 86, 1781-1788.

Yoon, H.C., Pozivil, P., Steinfeld, A., 2012. Thermogravimetric Pyrolysis and Gasification of Lignocellulosic Biomass and Kinetic Summative Law for Parallel Reactions with Cellulose, Xylan, and Lignin. Energ. Fuel. 26, 357-364.

Yu, H., Zhang, Z., Li, Z., Chen, D., 2014. Characteristics of tar formation during cellulose, hemicellulose and lignin gasification. Fuel 118, 250-256.

Zhou, H., Long, Y., Meng, A., Li, Q., Zhang, Y., 2013. The pyrolysis simulation of five biomass species by hemi-cellulose, cellulose and lignin based on thermogravimetric curves. Thermochim. Acta 566, 36-43.

Zhou, H., Meng, A., Long, Y., Li, Q., Zhang, Y., 2014a. Classification and comparison of municipal solid waste based on thermochemical characteristics. J. Air Waste Manage. 64, 597-616.

Zhou, H., Meng, A., Long, Y., Li, Q., Zhang, Y., 2014b. An overview of characteristics of municipal solid waste fuel in China: Physical, chemical composition and heating value. Renew. Sust. Energ. Rev. 36, 107-122.

Figure Captions

Fig. 1. Schematic diagram of the pyrolysis reaction system.

Fig. 2. PAH from the pyrolysis of different samples.

Fig. 3. Percentage of PAH with different number of rings.

Fig. 4. Mechanisms of coniferyl alcohol degradation.

Fig. 5. Mechanisms of PVC degradation to form PAH (Jordan et al., 2001).

Fig. 6. HACA reactions from naphthalene.

Fig. 7. Reaction of naphthalene and CPD to generate PAH.

Fig. 8. Formation of PAH from CPD and indene.

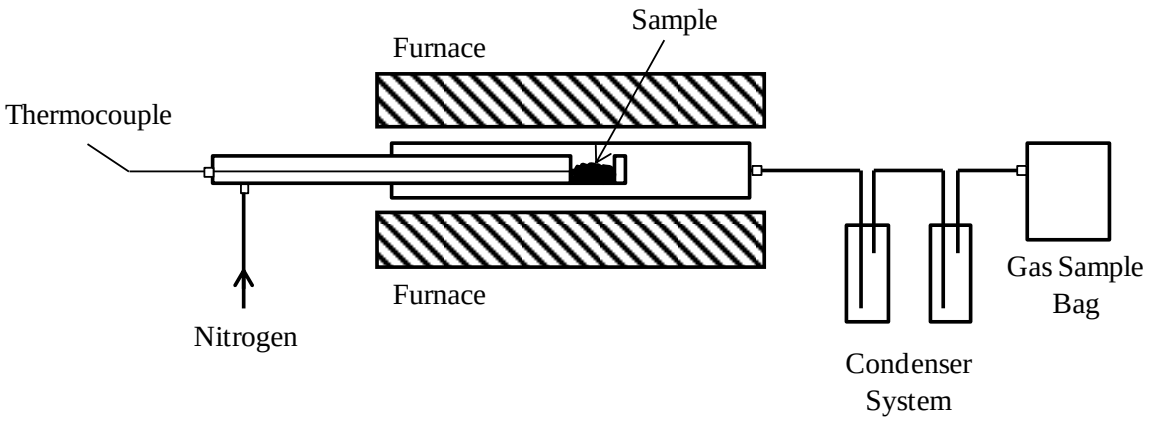

Fig. 1. Schematic diagram of the pyrolysis reaction system.

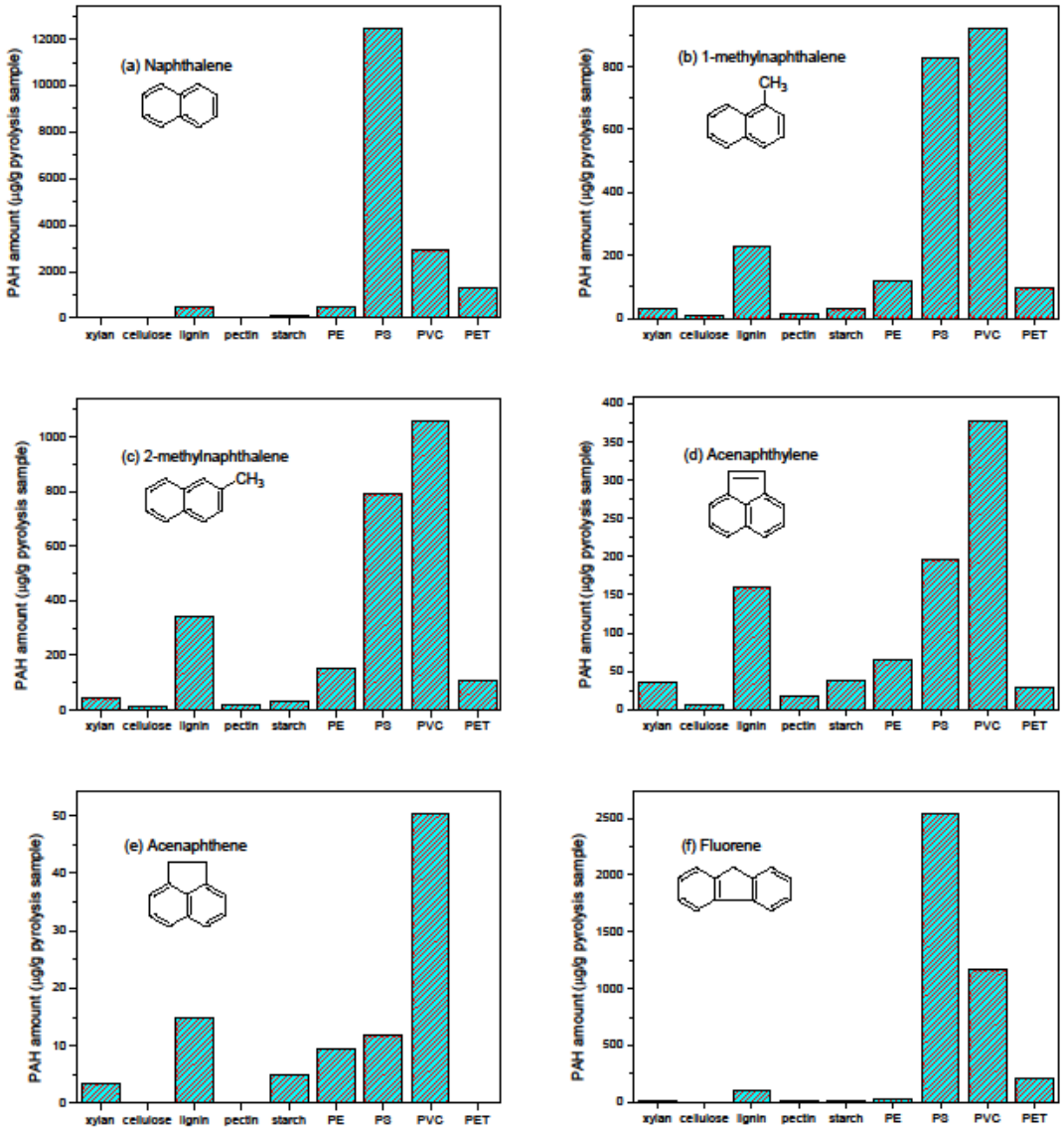
(a) Naphthalene
(b) 1-methylnaphthalene
CH3
(c) 2-methylnaphthalene
CH3
(d) Acenaphthylene
(e) Acenaphthene
(f) Fluorene
PAH amount (μg/g pyrolysis sample)
xylan
cellulose
lignin
pectin
starch
PE
PS
PVC
PET

Fig. 2

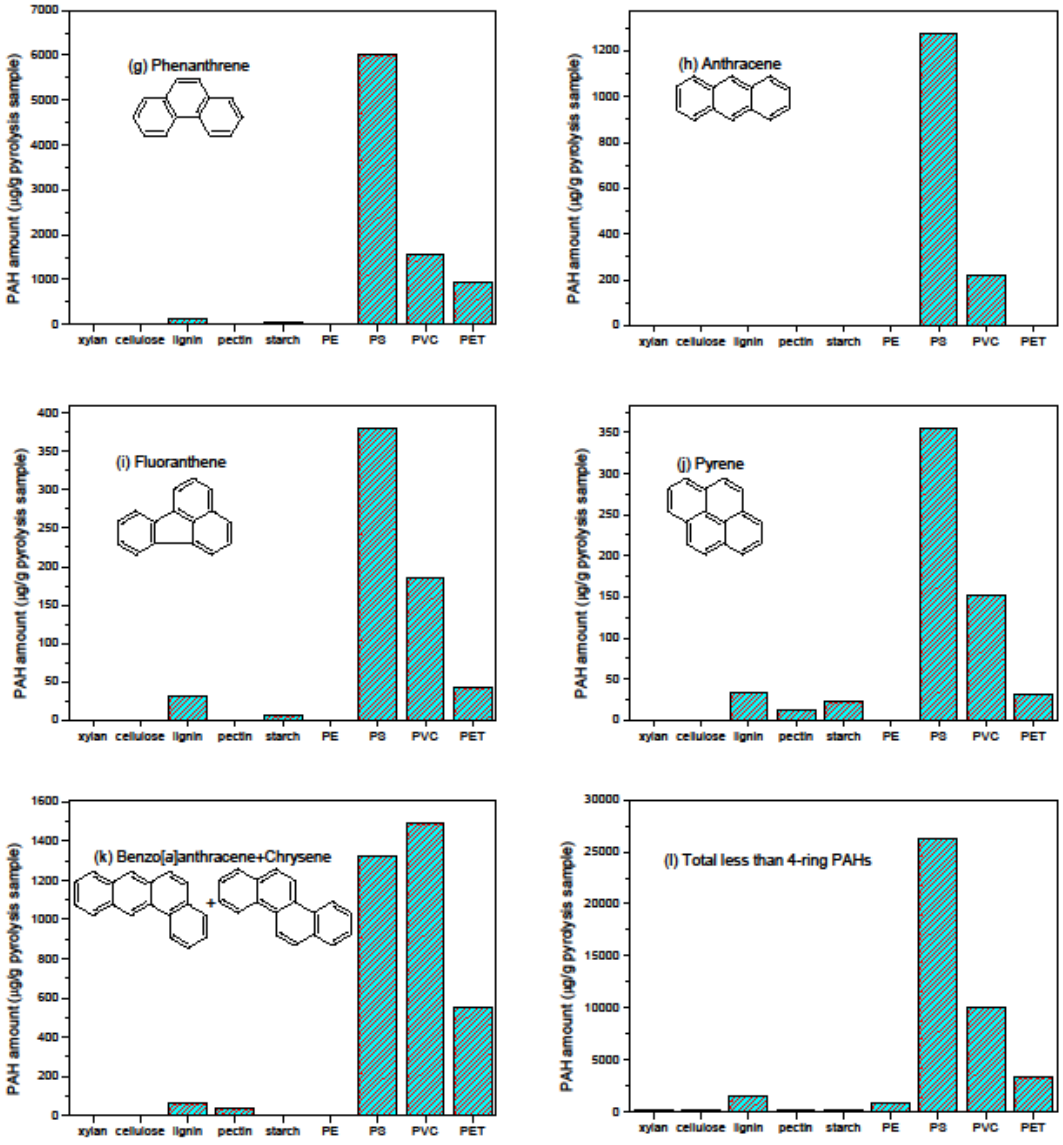

Fig. 2. PAH from the pyrolysis of different samples.

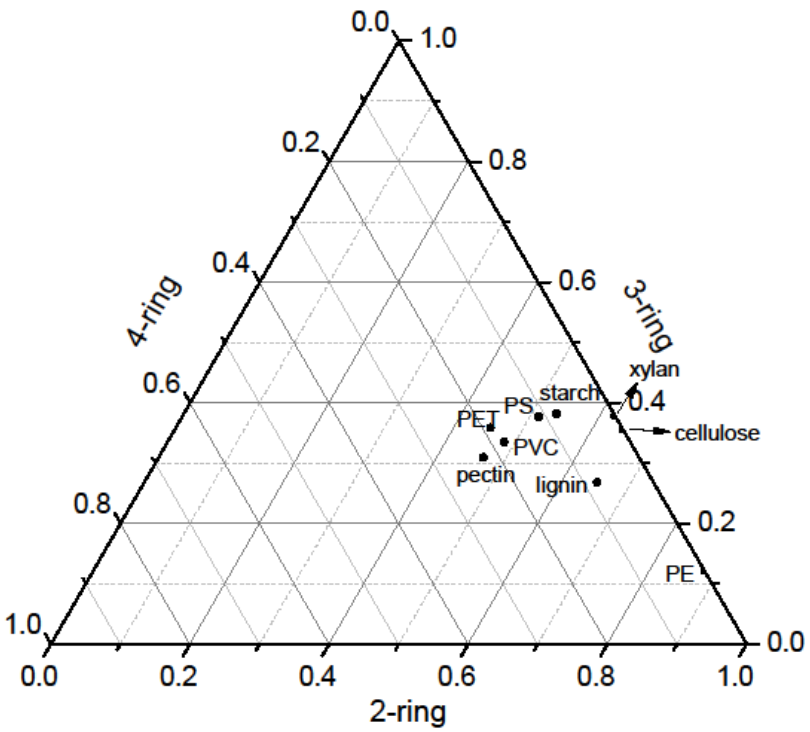

Fig. 3. Percentage of PAH with different number of rings.

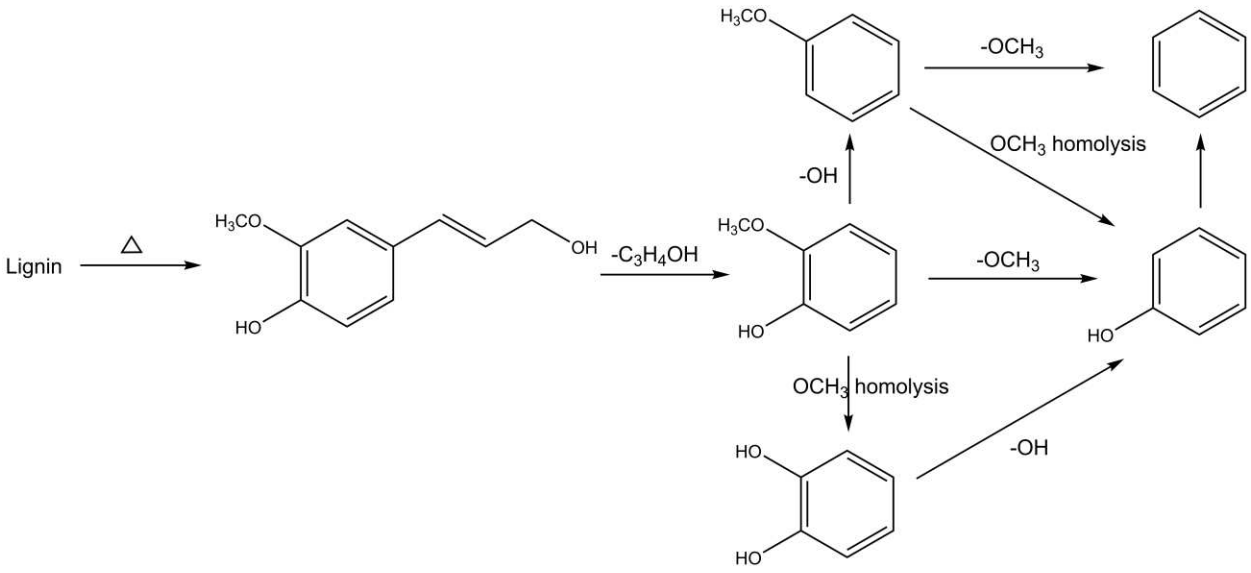

Fig. 4. Mechanisms of coniferyl alcohol degradation.

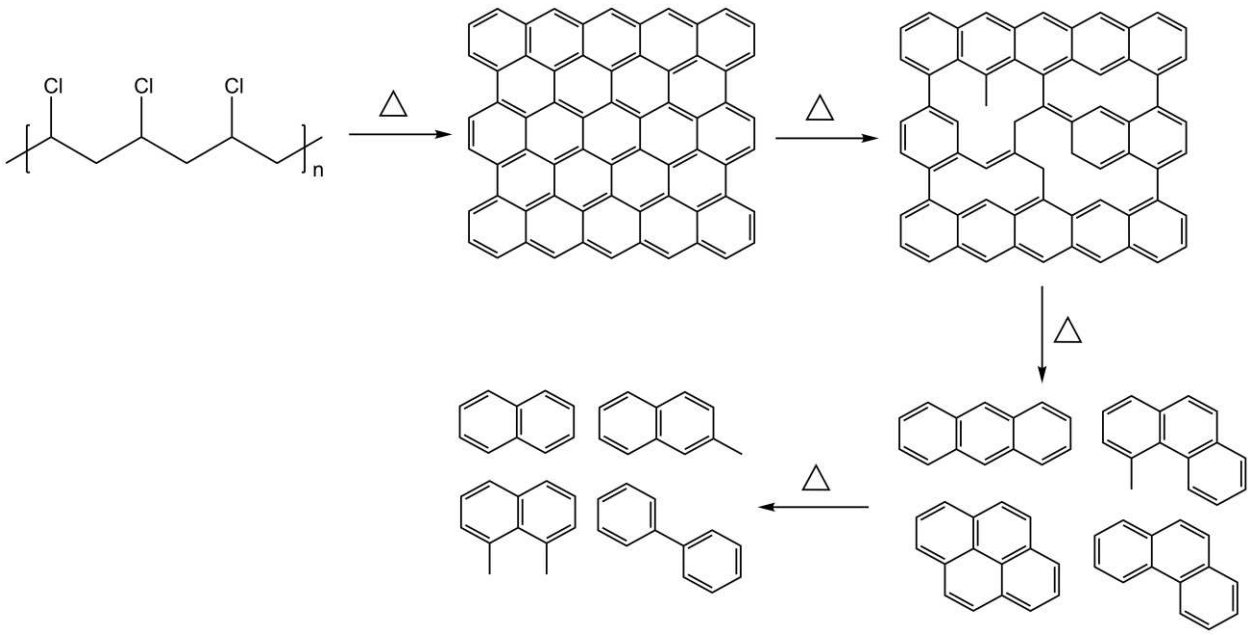

Fig. 5. Mechanisms of PVC degradation to form PAH (Jordan et al., 2001).

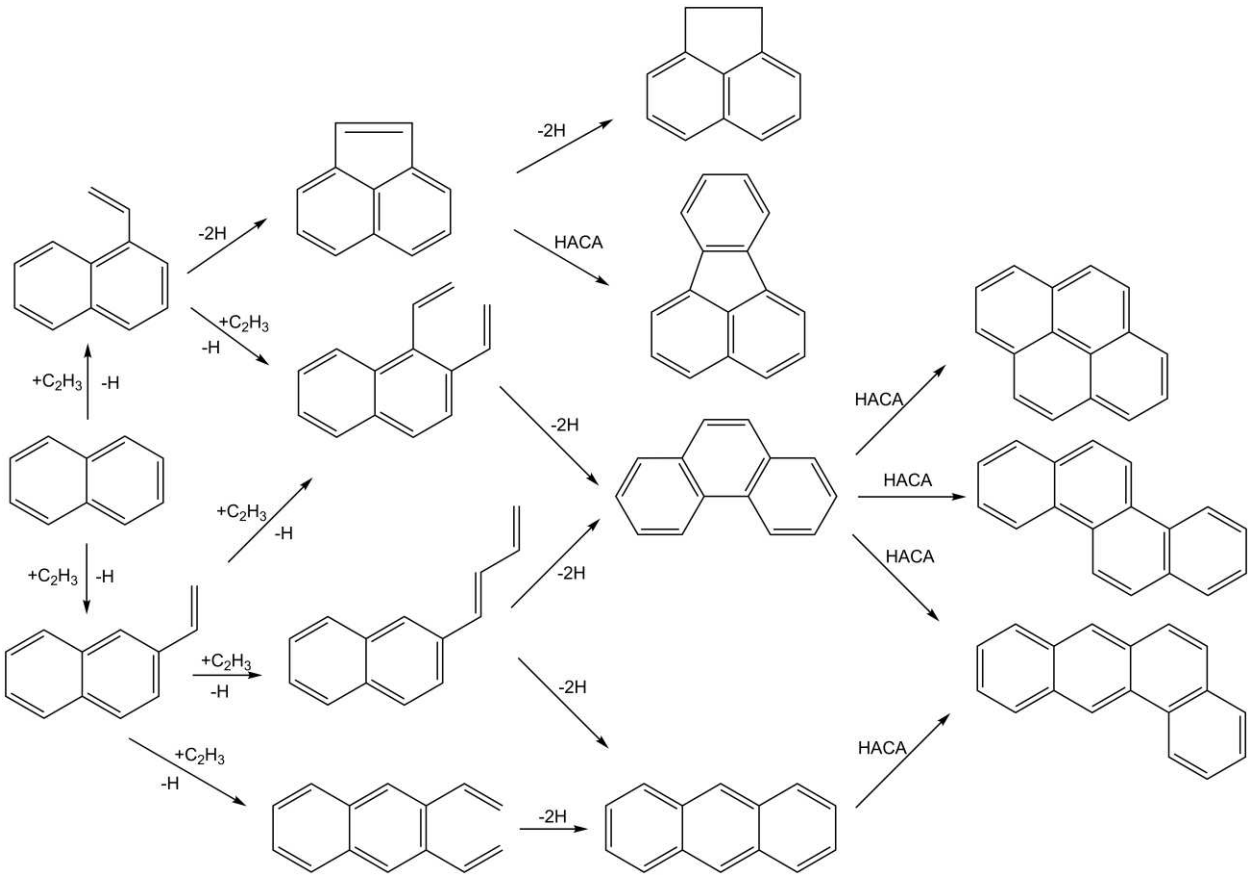

Fig. 6. HACA reactions from naphthalene.

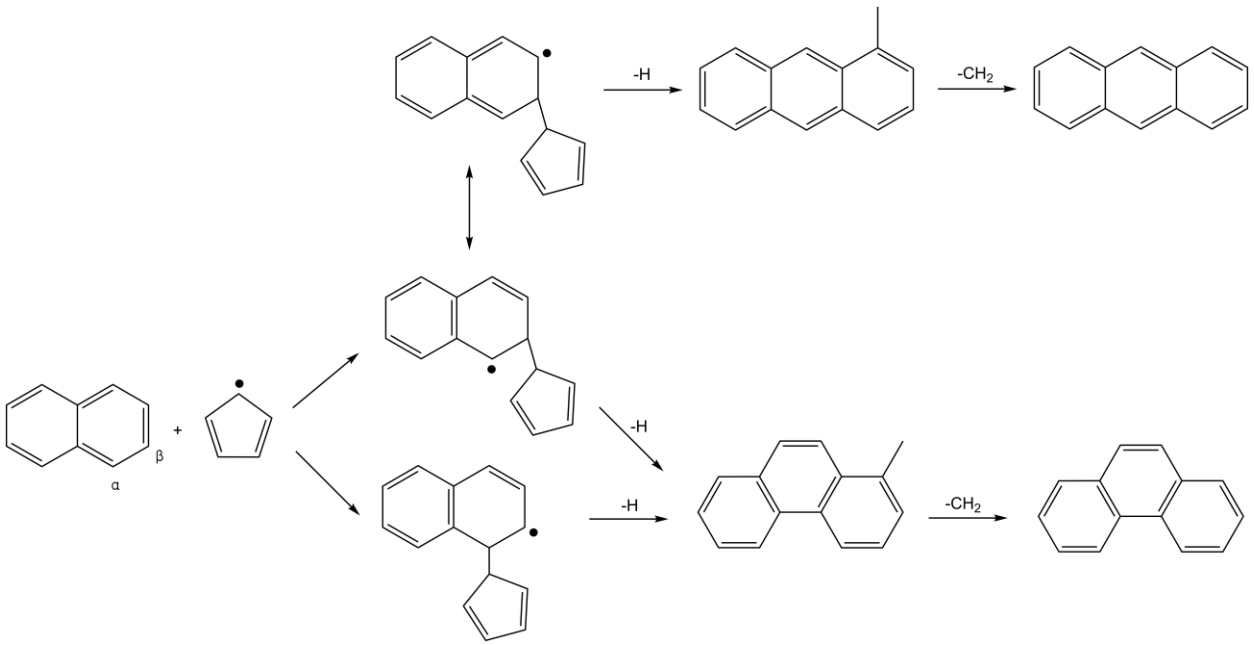

Fig. 7. Reaction of naphthalene and CPD to generate PAH.

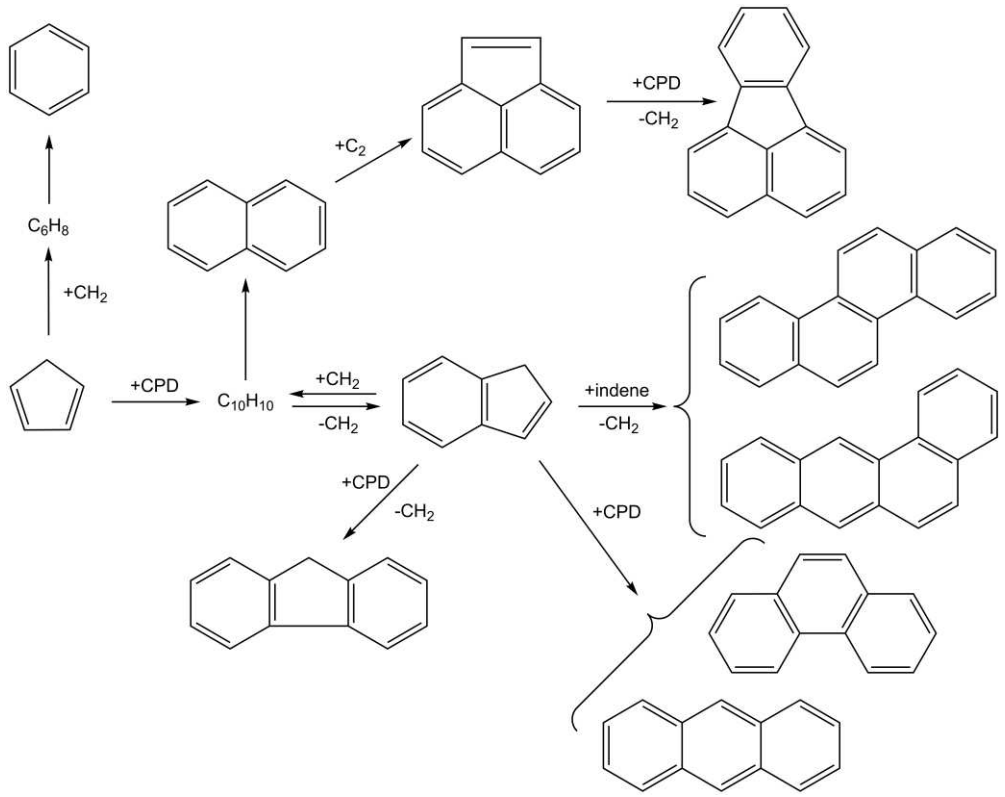

Fig. 8. Formation of PAH from CPD and indene.

Table 1. Proximate and ultimate analysis of different samples

Samples	Proximate Analysis[ar] (wt.%)				Ultimate Analysis[daf] (wt.%)					
	Moisture	Ash	Volatile	Fixed carbon	C	H	O	N	S	Cl
Xylan	5.83	3.61	77.79	12.78	40.26	5.49	51.55	2.70	-	-
Cellulose	4.67	0.07	93.37	1.89	41.66	5.71	52.20	0.41	0.02	-
Lignin	3.41	3.62	60.37	32.60	61.33	5.14	31.71	1.13	0.69	-
Pectin	8.01	3.11	68.56	20.32	44.25	4.97	50.14	0.48	0.16	-
Starch	12.07	0.12	83.71	4.10	43.83	5.21	50.56	0.20	0.19	-
PE	0.17	-	99.81	0.02	85.98	11.20	2.44	0.21	0.17	-
PS	0.45	0.04	99.12	0.39	86.06	6.27	1.74	5.73	0.19	-
PVC	0.16	-	94.78	5.06	38.34	4.47	-	0.23	0.61	56.35
PET	0.38	0.09	90.10	9.43	62.93	4.26	32.64	0.04	0.13	-

[ar]: as received basis; [daf]: dry ash free basis.

Table 2. Mass balance for the pyrolysis of various samples

	xylan	cellulose	lignin	pectin	starch	PE	PS	PVC	PET
Gas yield (wt.%)	44.8	60.7	30.4	44.3	62.2	46.3	5.7	44.4	47.2
Tar yield (wt.%)	37.6	28.2	25.8	32.3	30.8	42.6	84.3	31.3	38.2
Residue (wt.%)	17.8	4.9	33.3	25.3	7.7	0.0	2.3	15.6	4.5
Mass Balance[a] (wt.%)	100.2	93.8	89.5	101.9	100.7	88.9	92.3	91.3	89.9

[a] Mass balance was calculated as the mass of outputs (tar + gas + residue) divided by the mass of sample.